Heavy boson production via *ep* collisions at CERN LEP and LHC energies

A. Gutiérrez and A. Rosado
Instituto de Física, Universidad Autónoma de Puebla, Apdo. Postal J-48, Col. San Manuel, Puebla, Pue. 72570, Mexico
(Received 2 September 1997; published 19 February 1998)

We discuss the production of a heavy boson in deep inelastic e^-p scattering in the context of the standard model $SU(3)_C \times SU(2)_L \times U(1)$ of the strong and electroweak interactions at CERN LEP and LHC energies. We present results for the total and differential cross sections in terms of the parameters of the outgoing lepton. In addition to the γ-exchange diagrams we have also considered the contributions of $W^\pm$ and Z^0 exchange. They are found to be non-negligible, especially for the process $e^-p \to \nu_e W^- X$. We also present results for the energy spectrum and the angular distribution of the produced Z^0. Energy and angular distributions for Z^0 production are found to be strongly peaked, which will allow a clear identification of the produced Z^0. [S0556-2821(98)02505-3]

PACS number(s): 13.60.Hb, 13.85.Qk, 14.70.Fm, 14.70.Hp

I. INTRODUCTION

The CERN e^+e^- collider LEP and Large Hadron Collider (LHC) will provide us with the possibility to observe e^-p collisions with a maximal energy $E^{\max}=60$ GeV of the electron and $E_P^{\max}=7$ TeV of the proton [1]. A particularly interesting experiment at LEP and LHC will be electroproduction of weak bosons. One of the main goals at LEP and LHC is the exploration of physical frontiers beyond the standard model [2]. However, the rates of events for most of the exotic processes are of the same order of magnitude or smaller [3] than the expected rates for heavy gauge boson production in e^-p scattering. Hence, even if the cross sections for heavy boson production are not large enough to allow for detailed investigations of the $W^\pm$ and Z^0 properties, their calculation is necessary. Only if $W^\pm$ and Z^0 production, which together lay down an important background for new physics, are completely known and characterized can the latter be successfully investigated. Therefore our aim in the present work is to discuss in detail the heavy boson production in deep inelastic e^-p scattering. This will be done by using the coupling between fermions and bosons as given by the standard model of the strong and electroweak interactions and the parton model [4] through the parton distribution functions reported by Botts *et al.* [5], which take into account scaling violations and the heavy quarks contribution.

Three types of reaction mechanisms are discussed: $W^\pm$ and Z^0 production at the lepton line, at the quark line and through the fusion diagrams with the non-Abelian coupling of the gauge bosons. Our calculations include, aside from γ-exchange, Z^0- and $W^\pm$-exchange diagram contributions and are thus complete.

The first estimate for $W^\pm$ and Z^0 production in e^-p scattering as given by Llewelyn-Smith and Wiik in 1977 [6]. More recently, other authors have reported more detailed calculations [7–15]. It is not possible to compare directly all of our results with those of the former papers because different cutoffs were applied. In Ref. [9] the total cross section for the reaction $e^-p \to \nu_e W^- X$ was calculated with a cutoff of $O(1)$ GeV^2 taking into account the γ-exchange contribution only. For an energy in the center of mass of 1296 GeV and our cutoffs we get $\sigma_T = 5.5\times 10^{-37}$ cm^2 to be compared with $\sigma_T = 5.05\times 10^{-37}$ cm^2 [9]. For the process $e^-p \to eZ^0X$, Gabrielli [9] found for the lepton vertex contribution $\sigma_{\rm lep} = 3.3\times 10^{-37}$ cm^2. By using the same parameters we get a similar result; namely $\sigma_{\rm lep} = 3.2\times 10^{-37}$ cm^2. In our calculations we have also included the hadron vertex contribution, $\sigma_{\rm had} = 2.6\times 10^{-37}$ cm^2.

We also present results for the differential cross section as a function of the dimensionless variables x and y in order to compare the productions from the leptonic vertex and the hadronic vertex. Kinematical regions are found where either the lepton or the hadron vertex contributions can be neglected.

One of the aims of LEP and LHC is to explore the physics beyond the standard model. For example, particles predicted by supersymmetry [16], subconstituent models [3] and others. This can be accomplished only if the results of the standard model are known in detail. Our discussion is thus complemented by presenting calculations for the energy spectrum and the angular distribution of the produced Z^0. It is found that for fixed x and y Z^0 is mainly produced in a small, well determined region of the phase space. The expressions for the kinematics of the production of a massive boson in deep inelastic lepton-nucleon scattering and a discussion on the influence of experimental cuts on the phase space of the produced particles are given in Ref. [17], plus the explicit calculation of the matrix elements and the differential cross section for polarized scattering.

This paper is organized as follows: In Sec. II we describe the calculation of the differential cross section for inclusive $W^\pm$ and Z^0 production. In Sec. III we present and discuss our results for the total cross section and differential cross section as a function of the dimensionless variables x and y for all the different reactions and reaction mechanisms which contribute to charged vector boson and neutral vector boson production in e^-p collisions. Section IV contains the results for the energy spectrum and the angular distribution of the produced Z^0. Our conclusions are summarized in Sec. V.

II. THE DIFFERENTIAL CROSS SECTION FOR $W^\pm$ AND Z^0 PRODUCTION IN DEEP INELASTIC ELECTRON PROTON SCATTERING

A heavy boson $W^\pm$ and Z^0 can be produced in deep inelastic e^-p scattering via the following processes:

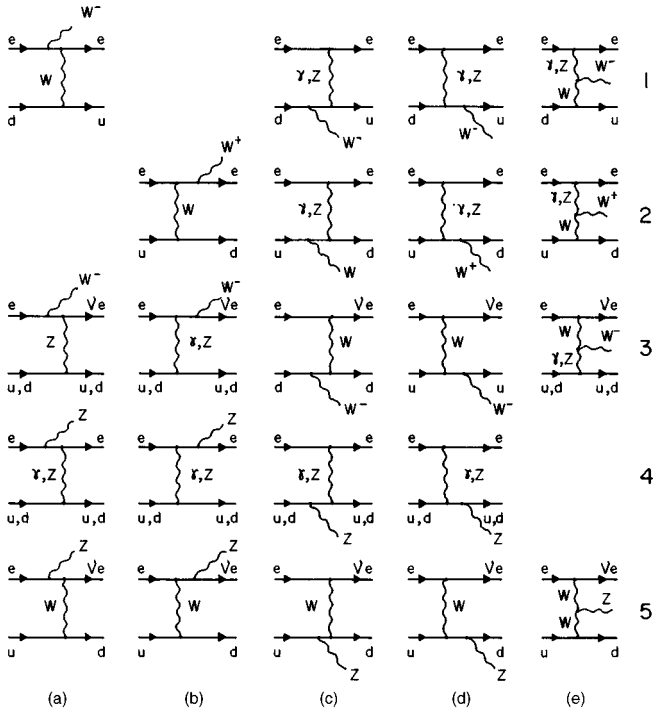

FIG. 1. Feynman diagrams which contribute to the amplitude of processes (1)–(5) at the lowest order in α; boson production from the initial (a) and final (b) lepton, the initial (c) and final (d) quark and through the non-Abelian couplings (e) (u stands for u, c, t, $\bar{d}$, $\bar{s}$, $\bar{b}$; d for d, s, b, $\bar{u}$, $\bar{c}$, $\bar{t}$).

$$e^- p \to e^- W^- X \tag{1}$$

$$e^- p \to e^- W^+ X \tag{2}$$

$$e^- p \to \nu_e W^- X \tag{3}$$

$$e^- p \to \nu_e W^+ X$$

$$e^- p \to e^- Z^0 X \tag{4}$$

$$e^- p \to \nu_e Z^0 X. \tag{5}$$

The diagrams which contribute at the lowest order in α at the quark level to the different reaction mechanisms (production at the leptonic vertex, at the hadronic vertex and through the boson self interaction) of all these processes are depicted in Fig. 1. The process $e^- p \to \nu_e W^+ X$ is forbidden at the lowest order in α.

We see from this figure that for reaction (5) only heavy boson exchange diagrams contribute and hence its cross section will be very small. In reaction (1) only quarks with isospin-1/2 whereas in reaction (2) and (5) only quarks with isospin 1/2 contribute.

We have discussed in detail Z^0 production and also the kinematics of heavy boson production in deep inelastic $e^- p$ scattering in the Ref. [17]. Notation and formulas as given in the latter to analyze the $W^\pm$ and Z^0 production are here adopted, though care is exercised with regard to the different ways in which the bosons are arranged in the non-Abelian coupling diagrams.

After the evaluation of the parton cross section $d\sigma^{l,q}$, we have to put them together with the parton distributions $f(x',\tilde{Q}^2)$ in order to evaluate the $e^- p$ cross section $d\sigma^{l,N}$. In Ref. [17] it has been pointed out that in contrast to ordinary deep inelastic scattering the choice of the effective momentum transfer square on the nucleon $\tilde{Q}^2$ is ambiguous in the case of the heavy vector boson production and dependent on the reaction mechanism. For leptonic production it is reasonable to take $\tilde{Q}^2 = -(p-p'-k)^2 = Q'^2$ since $p-p'-k$ is the momentum transfer to the nucleon (p,p' denote the four-momenta of the incoming and scattered electron, k the four-momentum of the produced boson). In the case of hadronic production the obvious choice is $\tilde{Q}^2 = -(p-p')^2 = Q^2$. For the non-Abelian diagrams a simple kinematical argument is not sufficient. For production of massive $W^\pm$ bosons in lepton quark scattering unitarity would not hold unless a coupling between the $W^\pm$, Z^0 and γ bosons is considered. This coupling occurs as a consequence of the gauge invariance of non-Abelian gauge theories. Therefore unitarity is restored through strong cancellations between these non-Abelian diagrams and either the leptonic [process (3)] or hadronic [processes (1) and (2)] contributions to lepton quark scattering. We propose a prescription which guarantees this gauge theory compensation also for the deep inelastic cross section: namely,

(a) $e^- p \to e^- W^- X$, $e^- p \to e^- W^+ X$

$$d\sigma^{l,N} = \sum_q \int dx' f_q(x',Q'^2) d\sigma_{ll}^{l,q} + \int dx' f_q(x',Q^2)(d\sigma_{hh}^{l,q} + d\sigma_{hn}^{l,q} + d\sigma_{nn}^{l,q}) + \int dx' \sqrt{f_q(x',Q^2)}\sqrt{f_q(x',Q'^2)} \times (d\sigma_{lh}^{l,q} + d\sigma_{ln}^{l,q}), \tag{6}$$

(b) $e^- p \to \nu W^- X$

$$d\sigma^{l,N} = \sum_q \int dx' f_q(x',Q'^2)(d\sigma_{ll}^{l,q} + d\sigma_{ln}^{l,q} + d\sigma_{nn}^{l,q}) + \int dx' f_q(x',Q^2) d\sigma_{hh}^{l,q} + \int dx' \sqrt{f_q(x',Q^2)}\sqrt{f_q(x',Q'^2)}(d\sigma_{lh}^{l,q} + d\sigma_{nh}^{l,q}), \tag{7}$$

(c) $e^- p \to e^- Z^0 X$, $e^- p \to \nu Z^0 X$

$$d\sigma^{l,N} = \sum_q \int dx' f_q(x',Q'^2)(d\sigma_{ll}^{l,q} + d\sigma_{ln}^{l,q} + d\sigma_{nn}^{l,q}) + \int dx' f_q(x',Q^2) d\sigma_{hh}^{l,q} + \int dx' \sqrt{f_q(x',Q^2)}\sqrt{f_q(x',Q'^2)}(d\sigma_{lh}^{l,q} + d\sigma_{nh}^{l,q}). \tag{8}$$

TABLE I. Contribution to the total cross sections from the different boson exchange diagrams: $E_e=60$ GeV, $E_P=7$ TeV.

Processes	$\sigma_\gamma(\text{cm}^2)$	$\sigma_{\gamma+Z}(\text{cm}^2)$	$\sigma_T(\text{cm}^2)$
$e^-p\to e^-W^-X$	5.7×10^{-36}	5.7×10^{-36}	6.1×10^{-36}
$e^-p\to e^-W^+X$	6.8×10^{-36}	6.8×10^{-36}	6.1×10^{-36}
$e^-p\to \nu W^-X$	4.6×10^{-37}	6.6×10^{-37}	5.5×10^{-37}
$e^-p\to e^-Z^0X$	5.5×10^{-37}	5.7×10^{-37}	5.8×10^{-37}
$e^-p\to \nu Z^0X$	0	0	1.4×10^{-37}

Summation is taken over all allowed quark and antiquark states: l,h,n denote leptonic, hadronic and non-Abelian, respectively.

In Eq. (6) the first line collects the expressions where the heavy boson is emitted from the lepton vertex using $f_q(x',Q'^2)$, the second line, production from the quark and the non-Abelian vertex with $f_q(x',Q^2)$, and the last one contains the contribution from the interference of these production mechanisms. In other words, contributions from diagrams with no γ or Z^0 exchange, from diagrams with γ or Z^0 exchange and interference terms are contained in the first, second, and third line in Eq. (6), respectively. In Eq. (7) the non-Abelian contribution arises together with the leptonic production since only this guarantees the required compensation. In Eq. (8) expressions where the heavy boson is emitted from the lepton line or the non-Abelian vertex, from the quark line, and interference of these production mechanisms, are contained in the first, second, and third line, respectively.

III. RESULTS FOR DEEP INELASTIC $W^\pm$ AND Z^0 PRODUCTION AT LEP AND LHC ENERGIES

In this section numerical results obtained by using the standard model of the electroweak interactions [2] are presented. We take $M_{Z^0}=91.2$ GeV and $M_W=80.3$ GeV for the masses of the neutral and charged bosons, and $\sin^2\theta_W=0.223$ for the electroweak mixing angle. We have included in our computations, in addition to γ-exchange, the Z^0-exchange, and the $W^\pm$-exchange diagrams. We present results for e^-p scattering with an electron energy $E=60$ GeV and a proton-energy $E_P=7$ TeV, i.e. in the LEP and LHC system. We take cuts of 4 GeV^2, 4 GeV^2, and 10 GeV^2 for Q^2, Q'^2, and the invariant hadronic mass square W, respectively. These values are suitable for the parton distribution functions of Botts *et al.* [5] and the latter are used in our calculations.

A. Total cross sections

Calculations that only take into account the contribution from photon exchange diagrams to the cross section of the processes (1)–(4) have been reported, where different parton distribution functions and cuts for the invariant mass square W are used. For the sake of comparison we give our results in Table I for the following cases: γ-exchange contribution σ_γ; γ- and Z^0-exchange contribution $\sigma_{\gamma+Z}$; and γ-, Z- and $W^\pm$-exchange contribution σ_T.

As expected, the dominant contributions to the total cross sections stem from photon exchange.

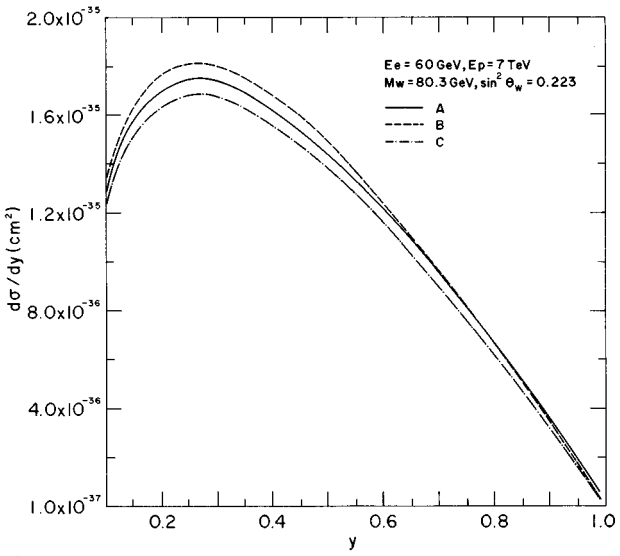

FIG. 2. Comparison of the contribution to $d\sigma/dy$ from the different boson-exchange diagrams for process (1). Curve C: only γ-exchange contribution; curve B: γ- and Z^0-exchange contribution; curve A: γ-, Z^0- and $W^\pm$-exchange contribution ($\sqrt{s}=1{,}296$ GeV).

B. $d\sigma/dy$ and $d\sigma/dxdy$

In Figs. 2–4 we compare $d\sigma_\gamma/dy$, $d\sigma_{\gamma+Z}/dy$, and $d\sigma_{\gamma+Z+W}/dy$ for the processes (1)–(3). From these plots it can be seen the importance of taking into account Z^0- and $W^\pm$-exchange contributions to $d\sigma/dy$ for $0.1\leqslant y<1$. In Figs. 5–7 we show in logarithmic scale the y dependence of the separated contributions of the lepton vertex, quark vertex and non-Abelian diagrams as well as the overall contributions. In Figs. 5 and 6 contribution of the quark vertex and non-Abelian diagrams is shown while in Fig. 7 contributions of the lepton vertex and non-Abelian diagrams are depicted. These plots illustrate the compensation mechanism characteristic of the non-Abelian structure of the electroweak stan-

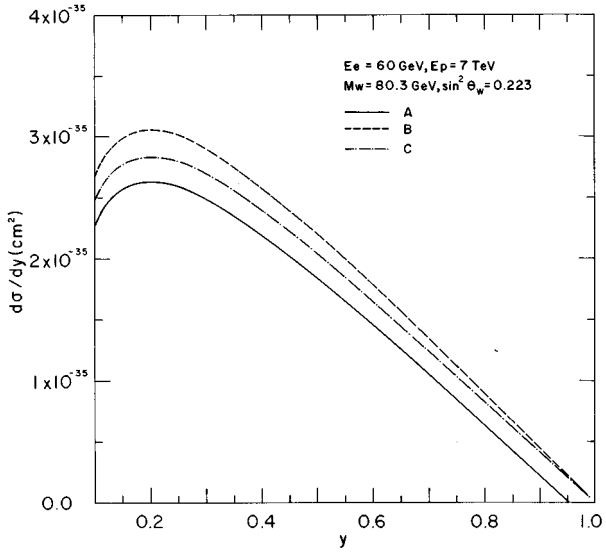

FIG. 3. Same as in Fig. 2, but for process (2).

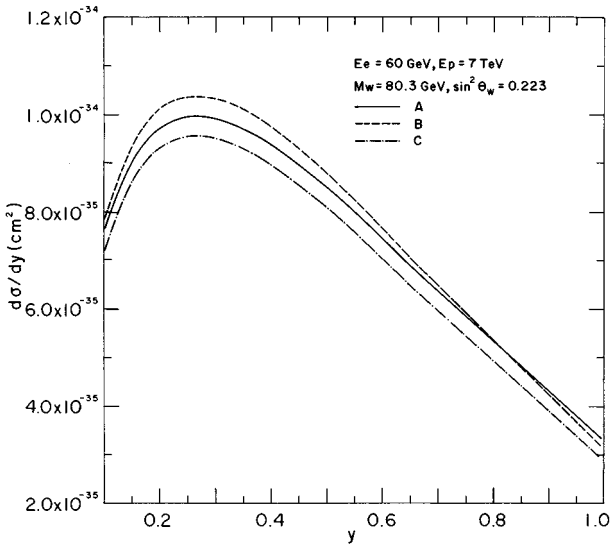

FIG. 4. Same as in Fig. 2, but for process (3).

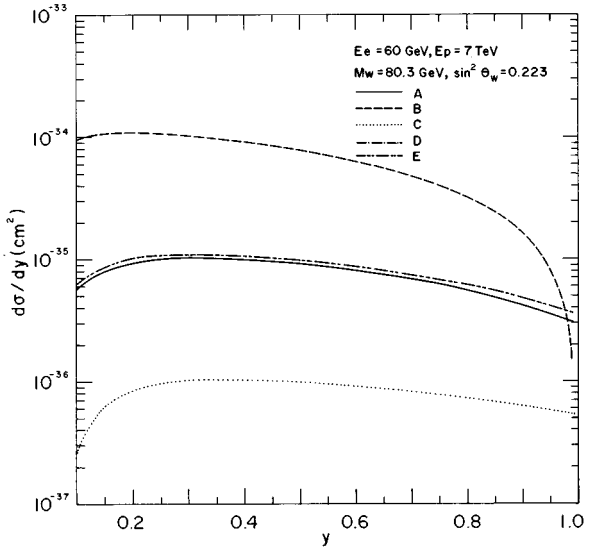

FIG. 6. Same as in Fig. 5, but for process (2).

dard model as a gauge theory. In process (3) this compensation reaches two orders of magnitude at LEP and LHC energies. Therefore, even small deviations of the coupling estructure from the standard model, like anomalous moment terms, can be expected to lead to observable deviations on results obtained through the standard model.

In Fig. 8 process (4) is shown in a logarithmic scale by depicting the y dependence of the quantities $d\sigma/dy$, $d\sigma_{\rm lep}/dy$, and $d\sigma_{\rm had}/dy$. In this figure the leptonic vertex contribution can be seen to increase steeply as y goes to 1 and thus becomes a dominant feature in $\sigma_{\rm tot}$.

In the same figure the sign of the contribution arising from the interference term is seen to be positive throughout.

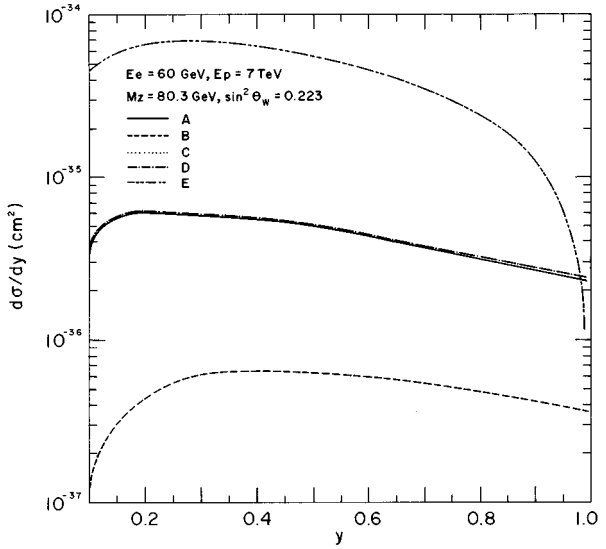

FIG. 5. Comparison of the contribution to $d\sigma/dy$ from the different boson production mechanisms for process (1). Curve A: total contribution; curve B: production at the leptonic vertex; curve C: production at the hadronic vertex; curve D: production through the non-Abelian couplings; curve E: sum of the hadronvertex and non-Abelian production mechanisms ($\sqrt{s}=1{,}296$ GeV).

We can also observe that for $y\approx 1$ the contribution from the leptonic clearly dominates, whereas for $y\approx\mu$ the hadronic production becomes the most important feature.

Our results for the dependence on x and y of the leptonic and hadronic contribution and the interference between them are shown in Fig. 9. The interference phase can also be seen to depend on variable x. We conclude from these figures that for $x\geq 0.1$ and $y\geq 0.95$ ($Q^2\geq 159{,}600$ GeV^2) production from the hadronic vertex can be safely neglected.

The main contribution to the Z^0 production from the leptonic vertex stems from the diagram in which the Z^0 boson is emitted by the initial electron [Fig. 1, Diagram 4(a)]. It is so because in this diagram the propagator of the virtual electron goes as $1/(p-k)^2$ whereas in that of [Fig. 1, Diagram 4(b)] (Z^0 boson emitted by the final electron) the corresponding propagator behaves as $1/(p+k)^2$.

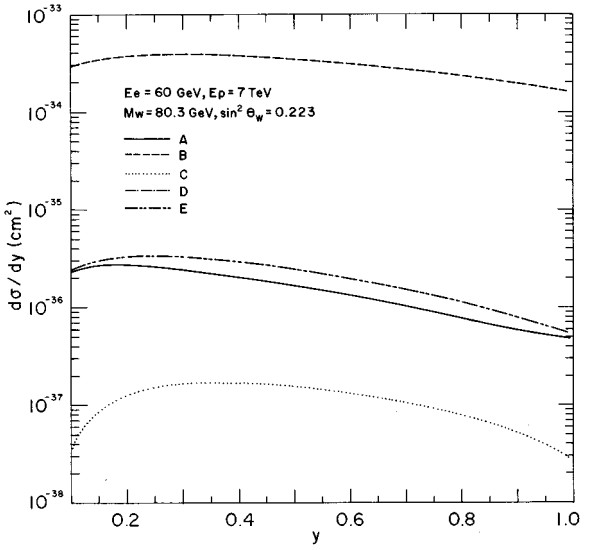

FIG. 7. Similar as in Fig. 5, but for process (3); here curve E is the sum of the lepton vertex and non-Abelian production mechanisms.

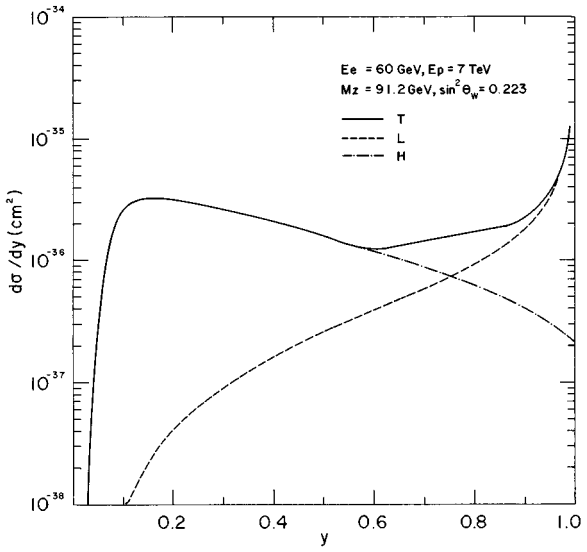

FIG. 8. $d\sigma/dy$, $d\sigma_{\rm lep}/dy$ and $d\sigma_{\rm had}/dy$, for $\sqrt{s}=1{,}296$ GeV.

The qualitative behavior of the leptonic contribution can be understood as follows. In Sec. II of the Ref. [17] it is seen that a cut on the invariant mass W induces a cut on the momentum transfer square of the exchanged boson, Q'^2. This cut depends on x and y (see Eq. 2.16 in Ref. [17]) and attains its minimal value at $x+\mu/y=0$ whereas it becomes large when $x+\mu/y$ approaches one. In other words, the most important contributions to the Z^0 production from the leptonic vertex are given by $x\sim 0$ and $y\sim 1$. The pronounced increase of this contribution observed in Fig. 8 when y goes to 1 can be explained as follows: The explicit form of the momentum transfer square of the exchanged electron in [Fig. 1, Diagram 4(a)], expressed in dimensionless variables, is $(p-k)^2=-s(1-y-\tau+y')$. However, from Eq. (2.9) in Ref. [17] it follows that $\tau^+\approx\tau^-\approx y'(1-x')$ for $y\approx 1$, hence $1/(p-k)^2\approx 1/sx'y'=1/Q'^2$. Note that the cross section is not necessarily zero in the limit $\tau^-=\tau^+$, because it contains integrals of the form

$$\int_{\tau^-}^{\tau^+}\frac{d\tau f(\tau)}{\sqrt{(\tau^+-\tau)(\tau^-\tau)}}$$

whose limit is $\pi\, f(\tau_0)$ for $\tau^-\to\tau^+=\tau_0$.

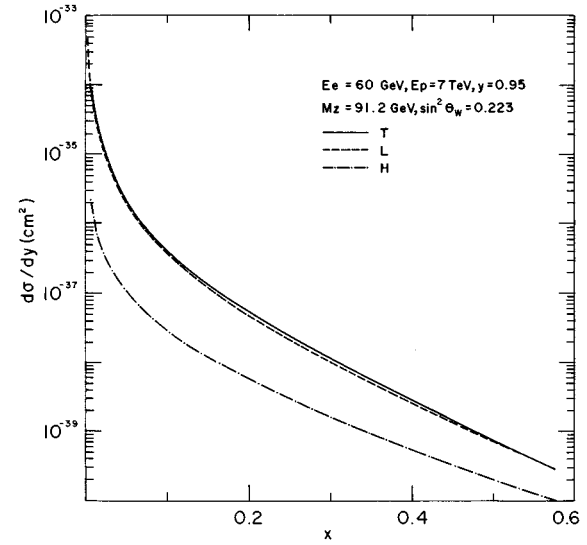

FIG. 9. $d\sigma/dxdy$ as function of x for $y=0.95$ $\sqrt{s}=1{,}296$ GeV. Shown are again the leptonic (curve L), hadronic (curve H), and total (curve T) cross sections.

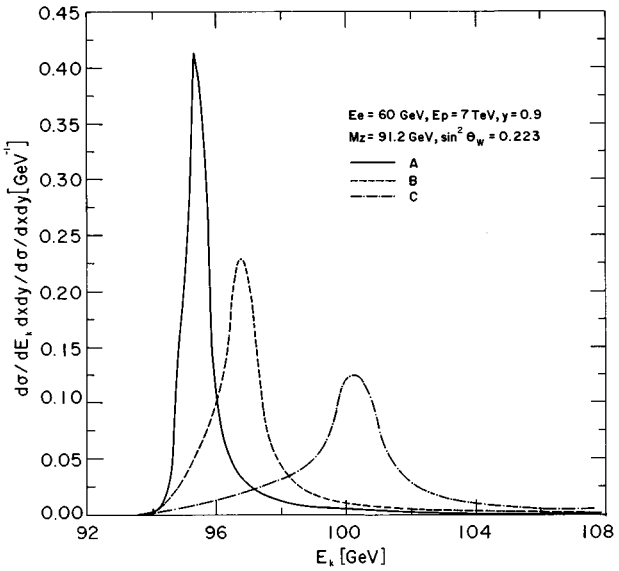

FIG. 10. Normalized energy spectrum of the produced Z^0 bosons for $y=0.9$ and $x=0.001$ (curve A), $x=0.003$ (curve B), $x=0.008$ (curve C) ($\sqrt{s}=1{,}296$ GeV).

We observe that the contribution to the Z^0 production from the hadronic vertex dominates for small x and y. This is due to the fact that the propagator of the exchanged photon in the contributing diagrams depicted in Fig. 1, Diagram 4(c) and Fig. 1, Diagram 4(d) behaves as $1/Q^2=1/sxy$. In this case, the propagator of the virtual quark in the diagram of Fig. 1, Diagram 4(c) (Z^0 boson emitted by the initial quark) behaves as $1/(q-k)^2$ and approaches $-1/Q^2$ when $y\to\mu$ $[(q-k)^2=\mu-x'(y-y')]$. However, in Fig. 8 we do not observe the same behavior as in the leptonic case for $y\to 1$, because when $y\to\mu$ the allowed intervals for x, x' and y' vanish altogether.

IV. ENERGY AND ANGULAR DISTRIBUTION OF THE PRODUCED Z^0

Results for the normalized energy distribution $(d\sigma/dE_k dxdy)/(d\sigma/dxdy)$ of the Z^0 are illustrated in Fig. 10 for $x=0.001$, 0.003, 0.008 and $y=0.9$, and in Fig. 11 for $x=0.001$, 0.003, 0.008 and $y=0.95$. We see that these energy distributions have a resonancelike behavior, the Z^0 bosons being mainly produced in a small E_k interval. Something similar happens with the normalized angular distribution $(d\sigma/d\cos\theta_k dE_k dxdy)/(d\sigma/dE_k dxdy)$. Figures 12 and 13 show that the Z^0 is mainly found in the forward direction and that the $\cos\theta_k$ distribution develops a sharp peak before reaching its kinematical limit. We also observe that most of the Z^0 bosons are produced in the plane which is spanned by the momenta of the incoming and outgoing leptons i.e. $\cos\phi_k\approx 0$. The reason for these sharp energy and angular

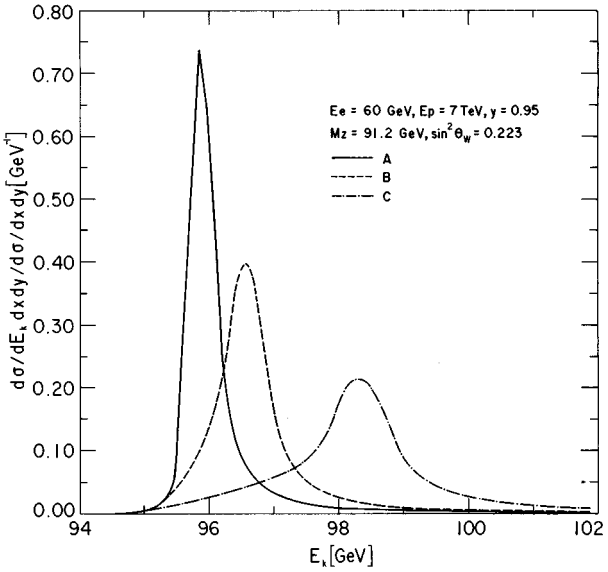

FIG. 11. Same as in Fig. 10, but with $y=0.95$ and $x=0.001$ (curve A), $x=0.003$ (curve B), $x=0.008$ (curve C).

distributions is that the differential cross section becomes large when $Q'^2=-(p-p'-k)^2$ approaches its minimal value, $Q'^2\approx Q'^2_{\rm cut}$. Then we have

$$x'\approx x+\mu/y$$

$$y'\approx Q'^2_{\rm cut}/(x+\mu/y)\approx 10^{-4}.$$

When these values for x', y' are substituted into the expression (2.9) of Ref. [17] we obtain

$$\tau\approx(1-x-\mu/y)(1-y).$$

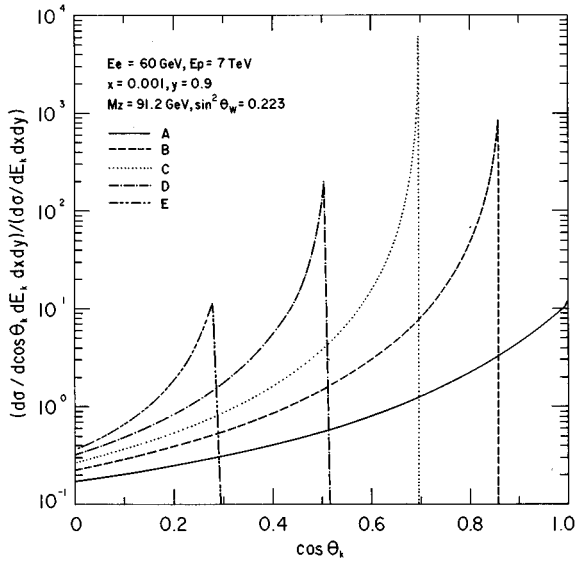

FIG. 12. Normalized angular distributions of the produced Z^0 bosons for $x=0.001$, $y=0.9$ and $E_k=94.5$ GeV (curve A), $E_k=95$ GeV (curve B), $E_k=95.5$ GeV (curve C), $E_k=96.5$ GeV (curve D), $E_k=99$ GeV (curve E).

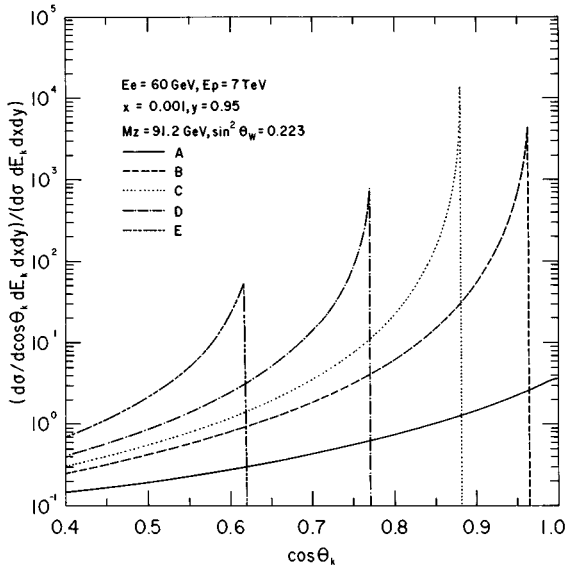

FIG. 13. Same as in Fig. 12, but for $x=0.001$, $y=0.95$ and $E_k=95$ GeV (curve A), $E_k=95.5$ GeV (curve B), $E_k=96$ GeV (curve C), $E_k=96.5$ GeV (curve D), $E_k=97.5$ GeV (curve E).

Then, by using Eq. (2.5) in [17] we obtain for $E_k^0(x,y)$ and $\cos\theta_k^0(x,y)$,

$$E_k^0(x,y)\approx Ey+E_p\mu/y+E_px(1-y), \tag{9}$$

$$\cos\theta_k^0(x,y)\approx(2Ey-E_k)/\sqrt{E_k^2-M_Z^2}, \tag{10}$$

associated with the maximal number of Z^0 bosons. These estimates are confirmed by accurate numerical evaluation. The last two expressions together with $\cos\phi_k\approx 0$ ($Q'^2\approx Q'^2_{\rm cut}$) for a given value of x and y (i.e. for a given energy and direction of the scattered electron) enables one to determine the region in the phase space where most of the Z^0 bosons can be found.

V. CONCLUSIONS

We have presented the complete calculation of heavy vector boson production in unpolarized deep inelastic e^-p scattering in the context of the standard model in conjunction with the parton model, at LEP and LHC energies.

By taking $M_W=80.3$ GeV, $M_{Z^0}=91.2$ GeV, $\sin^2\theta_W=0.223$, $\sqrt{s}=1{,}296$ GeV and by using the parton distributions reported by Botts *et al.*, a total production of about 290 Z^0, 3030 W^+, 3310 W^- bosons for an integrated luminosity of 500 pb^{-1}, for LEP and LHC was found.

We have included in our calculations Z^0-exchange and $W^\pm$-exchange diagrams, in addition to γ-exchange diagrams, where these contributions are found to amount to 6% of the photonic cross section. For the y distribution heavy boson exchange contributions were shown to be important, particularly for large values of y ($y\approx 1$).

Separate contributions from the different mechanisms of charged boson production were calculated. These lead to a compensation mechanism on the differential cross sections, which is typical of the non-Abelian structure of the electroweak standard model as a gauge theory. This compensa-

tion reaches up to two orders of magnitude at LEP and LHC energies. This means that even small deviations on the coupling structure of the standard model like anomalous magnetic moment terms will lead to detectable deviations in charged boson production in e^-p collisions. The decay of a neutral boson Z^0 into lepton pairs provides a clear signal of its production. Neutral bosons can be produced through neutral current and charged current interactions. The production rates for neutral current processes are expected to be larger than those for charged current processes because in the latter case photon-exchange diagrams do not contribute at the lowest order in α.

The contribution of the Z^0-exchange diagrams to the total cross section is a small percentage, where γ-exchange diagrams become by far the dominant ones. However, for large Q^2 and Q'^2 [i.e.,$O(M_Z^2)$] γ exchange as well as Z^0 exchange are important.

We compared the two production mechanisms, emission of the Z^0 at the leptonic vertex and at the hadronic vertex, and their interference. We found that there are kinematical regions where either the contribution from the leptonic vertex or that provided by the hadronic vertex can be neglected. The contribution to the cross section is mainly hadronic for $y \leqslant 0.5$ whereas for $0.8 \leqslant y < 1$ it is almost purely leptonic.

We also analyzed in the LEP and LHC system the energy E_k and $\cos\theta_k$ distributions of the produced Z^0 for a given x and y (i.e. for a given energy and polar angle of the final electron). Considering the region where the Z^0 production is almost purely leptonic, we found that the E_k and θ_k distributions are strongly peaked. It is shown that if the energy and polar angle of the scattered electron are given by scaling variables x and y, the boson Z^0 will be mostly produced with energy $E_k = Ey + E_p x(1-y) + E_p M_Z^2/(sy)$, polar angle $\cos\theta_k \approx (2Ey - E_k)/\sqrt{E_k^2 - M_Z^2}$ and azimuthal angle $\cos\phi_k \approx 0$.

Finally, it is worth mentioning that the resonancelike behavior of the E_k and θ_k distributions will help discriminate between the production of a standard Z^0 and the production of other particles, such as those predicted by theories dealing with other reaction mechanisms, for example supersymmetry [16] and subconstituent models [3], through experiments which will be carried at the collider LEP and LHC.

The cross section and consequently the even rate is presumably not large enough to allow for detailed investigation of the $W^\pm$ and Z^0 properties. However, it is of a comparable order or larger than that of many exotic processes. Therefore it is important to perform complete and detailed calculations of $W^\pm$ and Z^0 production since new physical features can be observed only if standard background events are correctly distinguished. In this sense the results of the present report may help clear the way toward new physics at LEP and LHC or future e^-p machines.

ACKNOWLEDGMENTS

Financial support from the *Consejo Nacional de Ciencia y Tecnología* (CONACyT) and *Sistema Nacional de Investigadores* (SNI) is gratefully acknowledged. We would like to thank A. Flores for careful reading of our manuscript.

[1] See e.g. R. Rückl, in *Large Hadron Collider Workshop*, Proceedings, Aachen, Germany, edited by G. Jarlskog and D. Rein (CERN Report No. 90-10, Geneva, Switzerland, 1990), and references therein.

[2] S. Weinberg, Phys. Rev. Lett. **19**, 1264 (1967); A. Salam, in *Elementary Particle Theory, Relativistic Groups and Analyticity (Nobel Symposium No. 8)*, edited by N. Svartholm (Almqvist and Wiksell, Stockholm, 1968); S.L. Glashow, J. Iliopoulos, and L. Maiani, Phys. Rev. D **2**, 1285 (1970).

[3] See e.g. R. J. Cashmore *et al.*, Phys. Rep. **22**, 277 (1985) and references therein.

[4] R. P. Feynman, *Photon-Hadron Interactions* (Benjamin, Reading, MA, 1972).

[5] J. Botts, J. G. Morfin, J. F. Owens, J. Qiu, W. K. Tung, and H. Weerts, Report No. Fermilab-Pub-92/371 (unpublished).

[6] C. H. Llewelyn-Smith and B. H. Wiik, DESY Report 77/36 (1977) (unpublished).

[7] P. Salati, and J. C. Wallet, Z. Phys. C **16**, 155 (1982).

[8] G. Altarelli, G. Martinelli, B. Mele, and R. Rückl, Nucl. Phys. **B262**, 204 (1985).

[9] E. Gabrielli, Mod. Phys. Lett. A **1**, 465 (1986).

[10] D. Atwood, U. Baur, G. Couture, and D. Zeppenfeld, Proceedings of the Snowmass DPF Summer Study 1988 (unpublished), p. 264.

[11] H. Baer, J. Ohnemus, and D. Zeppenfeld, Z. Phys. C **43**, 675 (1989).

[12] D. Atwood, U. Baur, D. Goddard, S. Godfrey, and B. A. Kniehl, Proceedings of the Snowmass DPF Summer Study 1990 (unpublished), p. 557.

[13] U. Baur, B. A. Kniehl, J. A. M. Vermaseren, and D. Zeppenfeld, Proceedings of the Aachen ECFA Workshop 1990 (unpublished), p. 956.

[14] U. Baur, J. A. M. Vermaseren, and D. Zeppenfeld, Nucl. Phys. **B375**, 3 (1992).

[15] U. Baur, Proceedings of the Rencontres de Moriond on QCD and High Energy Hadronic Interactions, Les Arcs, France 1992 (unpublished), p. 91.

[16] H. E. Haber and G. L. Kane, Phys. Rep. **117**, 75 (1985).

[17] M. Böhm and A. Rosado, Z. Phys. C **34**, 117 (1987).